SUPPLEMENTARY INFORMATION FOR
The nature of crack path instabilities in thin sheets cut by blunt objects

Eugenio Hamm[1], Iryna Sivak[2], Benoît Roman[3]
13 *Departamento de Física Universidad de Santiago de Chile, Avenida Ecuador 3493, 9170124 Estación Central, Santiago, Chile.*
[2] *École Polytechnique Fédérale de Lausanne, CH-1015, Switzerland.*
[3] *PMMH, CNRS, ESPCI Paris, Université PSL, Sorbonne Université, Université de Paris, F-75005, Paris, France.*

MODEL FOR CRACK PROPAGATION

We give here more detailed derivations of the results used in the main article.

Configuration $\mathcal{S}'$ - We show here a picture of the setup corresponding to configuration $\mathcal{S}'$, which defines the main geometric elements of the model.

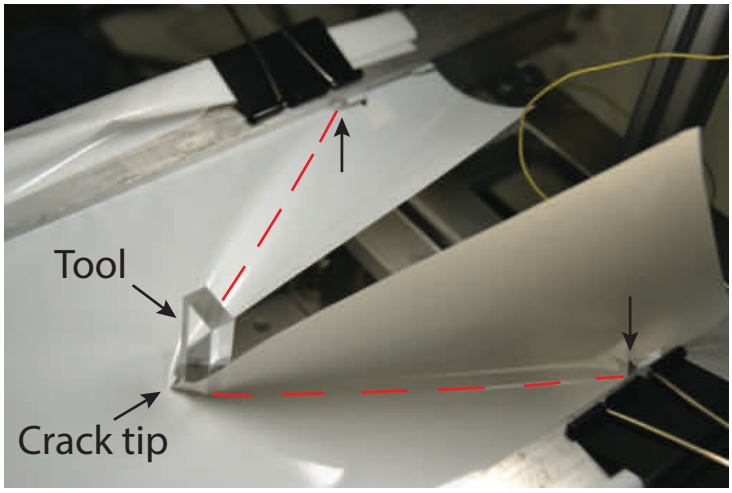

FIG. 1. Closeup of the setup corresponding to configuration $\mathcal{S}'$. Shown is the pushing tool that cuts the sheet, and the crack tip in front of the tool. Vertical arrows point to the cutting blades. The broken lines indicate the pushing lines on each side of the crack.

Elastic energy - The starting point is Equation (1) in the main article, the elastic energy of a thin sheet with thickness t, pushed along its edge with length l with a penetration angle α_l

$$U_l = aEtl^2 \tan^n \alpha_l. \tag{1}$$

Similar versions of this equation appeared in previous works [1–3] when deriving a model for crack propagation in a thin sheet that is pushed along a single edge. This expression was obtained within the assumption of small penetration angle $\alpha_l \ll 1$, and in [1–3] took the equivalent form $U_l = aEtl^2\alpha_l^n$. In this article we use $\tan\alpha \sim \alpha$ for the simplicity of calculations. Audoly et al. [2], assumed the exponent $n = 5$, whereas Vermorel et al. [3] argue that $n = 4$. We note that the difference in the choice of n will not change significantly the results, and choose here to follow the experimental fit of direct measurements by Romero et al. [1] ($n = 3.5, a = 0.0038$).

General energy for simultaneous loading - We extend the model to configuration $\mathcal{S}'$ that includes simultaneous contact with both left and right sides (see Fig.2a). The stretching energy is for each side

$$U_l = aEtl^2 \tan^n \alpha_l \qquad \text{and} \qquad U_r = aEtr^2 \tan^n \alpha_r. \tag{2}$$

The case illustrated in Fig. 2a corresponds to a crack that is strictly contained in $\mathcal{H}$, the convex hull of the crack path extending from the lower free edge (not shown), and the crack path described by the two cutting blades (not shown). Only the crack tip A is on the boundary of $\mathcal{H}$ and the angles α_l and α_r can be determined geometrically from the position of the crack tip and the tool. In this configuration we later derive analytic expressions from Eqs. (2) which further simplify by assuming that the low edge of the sheet is at infinity.

In the configuration of Fig. 2b, a finite portion of the crack path partly defines the boundary of $\mathcal{H}$. In general, the angles α_l and α_r are calculated from the set difference of $\mathcal{H}$ and $\tilde{\mathcal{H}}$, where $\tilde{\mathcal{H}}$ is the convex hull of the (crack path + tool). The set difference is shown as light grey regions in Fig. 2 and the penetration angle α_l (*resp.* α_r) are the angle difference of the left (*resp.* right) tangent to $\mathcal{H}$ and $\tilde{\mathcal{H}}$ at point A. Note also the corresponding definition for r in the same figure.

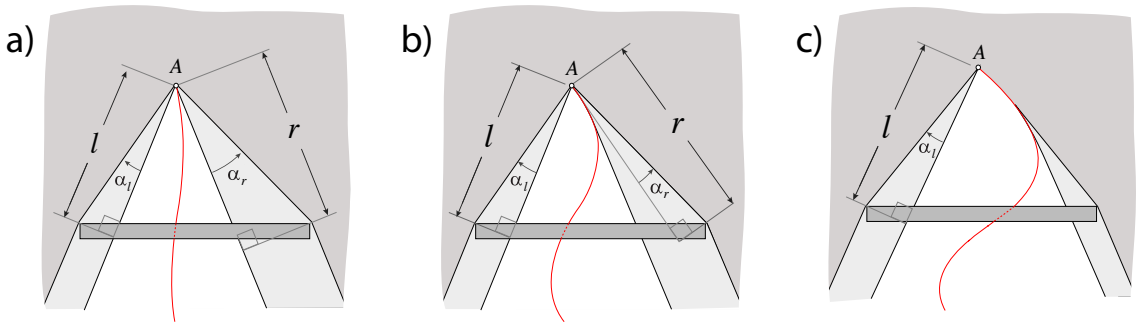

FIG. 2. Different configurations of crack propagation in configuration $\mathcal{S}'$: a) Crack path (red line) contained in the convex hull $\mathcal{H}$ (white region). b) Crack path contained in $\tilde{\mathcal{H}}$, the convex hull of $\mathcal{H}$ + the tool (shown in black). The set difference of $\tilde{\mathcal{H}}$ and $\mathcal{H}$ is shown in light grey. c) Hidden case in which the tool is hidden from the crack tip by its own path, and the right side of the crack does not contribute energetically to the propagation mechanism. In all cases angle α_r is measured from the set difference of $\tilde{\mathcal{H}}$ and $\mathcal{H}$.

Finally, in Fig. 2c, a finite length of the crack partly defines the boundary of $\tilde{\mathcal{H}}$. In the case represented, the angle $\alpha_r = 0$. We say in this case that the crack is "hidden" from the right pushing point. The right side contributes with no usable energy to the fracture process ($U_r = 0$) and the crack is driven only by the left side. The opposite case (left pushing point hidden) follows by symmetry. In this case $U_l = 0$.

Energy release rate - The energy release rate for the fracture in direction of unit vector $\mathbf{u}$, integrated over the thickness, is assumed to be simply the sum of the energy release rates for each side,

$$G(\mathbf{u}) = G_l(\mathbf{u}) + G_r(\mathbf{u}) = [\mathbf{F}_l \cdot \mathbf{u}]^+ + [\mathbf{F}_r \cdot \mathbf{u}]^+, \tag{3}$$

where $[x]^+ = (x + |x|)/2$ denotes the positive part of x, and

$$\mathbf{F}_l = -\nabla U_l \quad \text{and} \quad \mathbf{F}_r = -\nabla U_r, \tag{4}$$

are configurational forces associated to the release of energy only from the left side ($U_l = aEtl^2 \tan^n \alpha_l$) or from the right side ($U_r = aEtr^2 \tan^n \alpha_r$). When the two sides contribute to the energy available for crack propagation i.e. when both positive parts are non-zero, the energy release rate is $G = \mathbf{F}_t \cdot \mathbf{u}$, where $\mathbf{F}_t = \mathbf{F}_l + \mathbf{F}_r$ is the resultant configurational force. Equation (3) contains all possible propagation modes, namely when the crack is only driven by the left side, only by the right side, and by both sides.

Rules for crack propagation - Our model for crack propagation is based on the Griffith criterion and the *Maximum Energy Release Rate* (MERR) criterion. To determine at any stage the instantaneous propagation direction of the crack, we compute the maximum of G among all possible propagation directions $\mathbf{u}$ such that $G(\mathbf{u}) = \gamma t$. According to (3) we identify three modes of propagation: the crack may propagate either driven by the left side only when $[\mathbf{F}_r \cdot \mathbf{u}]^+ = 0$, only by the right side when $[\mathbf{F}_l \cdot \mathbf{u}]^+ = 0$, or driven by both sides when $[\mathbf{F}_l \cdot \mathbf{u}]^+ \neq 0$ and $[\mathbf{F}_r \cdot \mathbf{u}]^+ \neq 0$. The three modes are characterised by three corresponding local maxima of G: the actual propagation direction is the one corresponding to the global maximum.

Numeric implementation - To numerically compute crack paths we iteratively apply the rules for crack propagation. One iteration consists of the following steps:

1. Move the tool by a small increment.
2. Find $\mathcal{H}$, $\tilde{\mathcal{H}}$, and determine α_l and α_r from the set difference of $\mathcal{H}$ and $\tilde{\mathcal{H}}$.
3. Evaluate the energy of the system, according to (2), and the configurational forces $\mathbf{F}_l$, $\mathbf{F}_r$, $\mathbf{F}_t$.
4. Compute $G_{max} = \max\{||\mathbf{F}_l||, ||\mathbf{F}_r||, ||\mathbf{F}_t||\}$.
5. If $G_{max} < \gamma t$, then go to step 1.
6. If $G_{max} \geq \gamma t$, then move the crack by a small increment in the most favourable propagation direction according to step 4, and go to step 2.

In the numerics we use $\gamma/E = 4\mu$m, and $n = 3.5$, noting that any $3.5 \leq n \leq 5$ gives qualitatively similar results. For instance, Audoly *et al.* [2] use $n = 5$, while Vermorel *et al.* [3] use $n = 4$. The chosen value is consistent with direct experimental observations [1].

ANALYTICAL THRESHOLDS

We present here analytical expressions for the thresholds that characterise the hysteretical behaviour of the transition from straight to oscillatory in configuration $\mathcal{S}'$, and radial to spiral in the configuration $\mathcal{C}$. We restrict the analysis to a centered crack ($\alpha_l = \alpha_r \doteq \alpha$), strictly contained in $\mathcal{H}$ as in Fig. 2a. Moreover, we assume that the cutting blades are at infinity, a valid approximation as long as $w \ll W$ (w is the width of the tool, whereas W is the distance between the blades). We also define θ as the angle between the propagation vector $\mathbf{u}$ and the longitudinal direction (positive to the right). Using Eqs. (2-4), straightforward algebra leads to the following ERR's for each propagation mode:

$$G(\theta) = \frac{\gamma t}{\mu}\frac{\cos\alpha}{\cos(\psi-\alpha)}\tan^{n-1}\alpha \begin{cases} \frac{1}{2}\left[\cos(\theta+\psi) + \frac{n-2}{n}\tan\alpha\sin(\theta+\psi)\right], & \text{only left side } ([\mathbf{F}_r]^+ = 0) \\ \frac{1}{2}\left[\cos(\theta-\psi) - \frac{n-2}{n}\tan\alpha\sin(\theta-\psi)\right], & \text{only right side } ([\mathbf{F}_l]^+ = 0) \\ \left[\cos\psi + \frac{n-2}{n}\tan\alpha\sin\psi\right]\cos\theta, & \text{both sides} \end{cases} \tag{5}$$

where $\mu = \gamma/(anEw) \approx 0.02$. Now, from (5) we compute the local maxima of energy release rate and the corresponding propagation directions. In the case of a crack driven solely by the right or by the left pushing side,

$$G_{max} = \frac{\gamma t}{2\mu}\frac{\cos\alpha}{\cos(\psi-\alpha)}\tan^{n-1}\alpha\sqrt{1+\left(\frac{n-2}{n}\right)^2\tan^2\alpha} \tag{6}$$

$$\tan\theta = \pm\frac{n\tan\psi - (n-2)\tan\alpha}{n + (n-2)\tan\alpha\tan\psi}, \tag{7}$$

where the $+$ $(-)$ sign corresponds to the right (left) case. When the crack is driven by the two pushing sides the maximum energy release rate and corresponding propagation direction are

$$G_{max} = \frac{\gamma t}{\mu}\frac{\cos\alpha}{\cos(\psi-\alpha)}\tan^{n-1}\alpha\left(\cos\psi + \frac{n-2}{n}\tan\alpha\sin\psi\right) \quad \text{and} \quad \theta = 0. \tag{8}$$

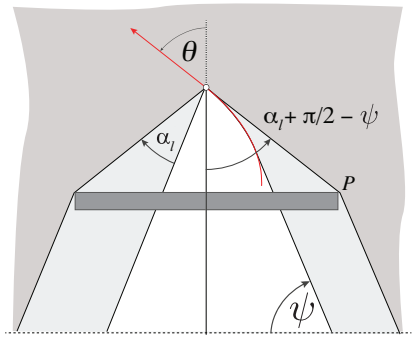

FIG. 3. Geometry for the computation of the absolute critical angle ψ_1 in the configuration $\mathcal{S}$.

Straight to oscillatory threshold ψ_2 - We derive the value of the control parameter ψ above which the straight propagation is no longer possible in configuration $\mathcal{S}'$, for an initially centered crack. In our model this occurs at a critical value ψ_2 such that the maximum energy release rate G_{max} becomes equal for one and two pushing sides. At the critical point, $G_{max} = \gamma t$ (Griffith criterion). Based on these considerations Eqs. (6) and (8) become

$$\frac{1}{2\mu}\frac{\cos\alpha}{\cos(\psi_2-\alpha)}\tan^{n-1}\alpha\sqrt{1+\left(\frac{n-2}{n}\right)^2\tan^2\alpha} = 1 \tag{9}$$

$$\frac{1}{\mu}\frac{\cos\alpha}{\cos(\psi_2-\alpha)}\tan^{n-1}\alpha\left(\cos\psi_2 + \frac{n-2}{n}\tan\alpha\sin\psi_2\right) = 1. \tag{10}$$

A numerical solution of this set of equations gives an equilibrium angle $\alpha = 13.53^\circ$ and a critical value of the control parameter, $\psi_2 = 65.61^\circ$. We note that the value of the threshold computed in this way differs from the value obtained in the numerics because in the latter the cutting blades are at a finite distance from the pushing tool.

It is instructive to seek for the solution of (9-10) in terms of powers of the small parameter α. To this end we develop the maxima of energy release rate, Eqs. (6) and (8), as

$$G_{max} = \frac{\gamma t}{2\mu\cos\psi}(1-\alpha\tan\psi)\alpha^{n-1} + \mathcal{O}(\alpha^{n+1}), \quad \text{(one side)} \tag{11}$$

$$G_{max} = \frac{\gamma t}{\mu}\left(1 - \frac{2\alpha}{n}\tan\psi\right)\alpha^{n-1} + \mathcal{O}(\alpha^{n+1}), \quad \text{(two sides)}. \tag{12}$$

To zeroth order, the condition $G_{max} = \gamma t$ implies $\psi_2 = \pi/3$. To first order in α, we assume that $\psi_2 = \pi/3 + \mathcal{O}(\alpha)$, and the same condition leads to

$$\psi_2 = \frac{\pi}{3} + \frac{n-2}{n}\alpha, \quad \text{with} \quad \alpha = \mu^{\frac{1}{n-1}},$$

hence to $\psi_2 \approx 65.14^\circ$.

Subcritical threshold ψ_1 (oscillatory case) - This threshold is intimately related to the hiding mechanism responsible for the observed oscillations, which at sufficiently small ψ are no longer possible. A rough estimate of the critical case is illustrated in Fig. 3, where the crack tip is initially at the center. If the crack started propagating to the left along direction θ, only driven by the left pushing side (for instance by imposing an initial condition consisting in an infinitesimal kink that forces the crack to move to the left), the pushing point P would become instantly hidden from the crack if $\theta > \alpha_l + \pi/2 - \psi$, and the crack would propagate a finite distance to the left, driven only by the left side, while the tool moves further. The critical condition for hiding occurs when the tangent to the crack path at the crack tip, drawn from P is aligned with the propagation direction θ at the onset of propagation. The value of α_l can be found from Eqs. (6-7) by enforcing the alignment condition $\theta = \alpha_l + \pi/2 - \psi$. The result is $\alpha_l \approx 14.07^\circ$ and $\psi_1 \approx 55.1^\circ$. A useful approximation can be obtained by solving to first order in the angle α_l,

$$\psi_1 = \frac{\pi}{4} + \frac{n-1}{n}\alpha_l.$$

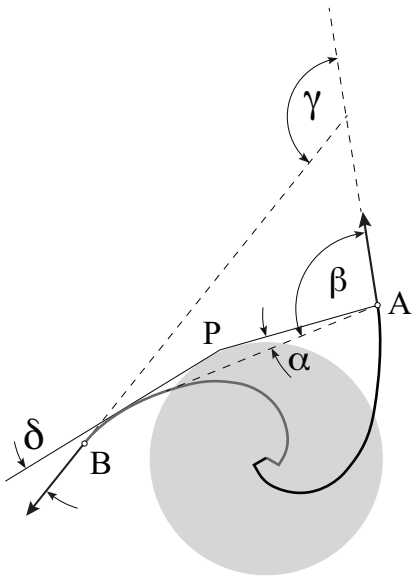

FIG. 4. Geometry for the computation of the absolute critical angle ψ_1 in the spiral case. The cone (grey circle) is pushing at point P

Subcritical threshold ψ_1 (spiral case) - As for the $\mathcal{S}'$ configuration we look for the hiding condition in the spiral geometry of configuration $\mathcal{C}$. In Fig. 4 the pushing point P is hidden from crack B, γ is the N-fold symmetry angle such that $\gamma = 2\pi/N$ (N continuous). We express γ in terms of the pushing angle α at the onset of crack propagation, the delay angle δ and the propagation angle $\beta = \pi/2 + [(n-2)/n]\alpha$ of crack A (see Fig. 4 for definitions and also Fuentealba *et al.* [4]), namely

$$\gamma \approx \alpha + \beta + \delta,$$

which is valid for small values of δ. Equality holds for a vanishing delay angle, $\delta = 0$, which is the sought critical condition for hiding. Noting that $\psi = \pi/N$ we may replace $\gamma = 2\psi$ and solve for ψ,

$$\psi = \frac{\pi}{4} + \frac{n-1}{n}\alpha,$$

which is equal to the threshold in the $\mathcal{S}'$ configuration.

[1] V. Romero, B. Roman, E. Hamm, and E. Cerda, Soft Matter **9**, 8282–8288 (2013).
[2] B. Audoly, P. -M. Reis, and B. Roman, Phys. Rev. Lett. **95**, 025502 (2005).
[3] R. Vermorel, N. Vandenberghe, and E. Villermaux, Phys. Rev. Lett. **104**, 175502 (2010).
[4] J. -F. Fuentealba, E. Hamm, and B. Roman, Phys. Rev. Lett. **116**, 165501 (2016).